Excerpt from the Proceedings of the 2011 COMSOL Conference in Bangalore

Design, Simulation and Study of MEMS Based Micro-needles and Micro-pump for Biomedical Applications

Pranay Kanti Podder[1], Dhiman Mallick[1] , Dip Prakash Samajdar[1], Anirban Bhattacharyya[1]
[1]Institute of Radio Physics and Electronics, University of Calcutta, Kolkata, WB, India
*Corresponding author: pranaypodder@gmail.com

Abstract: In this paper, we have addressed the issues related to the design and simulation of MEMS based silicon micro-needles for insertion of fluid into the dermis and subcutaneous fat layer of human skin. The cross-sectional areas of the needle bores were optimized considering the needle deflection and mechanical stress against flow rate in the channel. In addition, a poly-silicon micro-pump based on the principle of electrostatic actuation has been designed and simulated which can be integrated with the proposed micro-needles to control the fluid flow. The mechanical and fluidic models of the micro-needles and micro-pump were designed and simulated by using COMSOL MULTIPHYSICS v3.5.

Keywords: Micro-needle, Micro-pump, Electrostatic actuation, Diaphragm.

1. Introduction

1.1 Micro-needles

The major drawbacks of the conventional hypodermic needles are pain, risk of infection and the need of trained staff for the injection process. Also, conventional needles are not capable of sampling microscopic volume of fluids, which is often necessary in the world of lab-on-a-chip, which is the promising new technology that is expected to revolutionize medical diagnostic processes. With the advent of the MEMS (Micro Electro Mechanical Systems) technology, micro-machined hollow micro-needles can be fabricated, which can serve the purpose of extraction and insertion of micro-volumes of fluids with minimal invasion of tissue, and thus causing little or no pain [1,3].

1.2 Micro-pumps

Need for controlled fluid flow, for various medical applications have motivated research in MEMS based micro pumps. Their various uses are in controlled biological fluid flow for PCR (polymerase chain reaction) in DNA analysis, lab-on-a-chip devices, micro-total analysis systems (μTAS), and drug delivery systems [2]. Other applications for such devices are in micro-pump and micro-channel based liquid cooling mechanisms for electronic integrated circuits.

By integrating diagnostic as well as therapeutic functionalities, micro-needles and micro-pumps will be capable of personalized drug delivery in response to a patient's specific health conditions.

2. Device Design

2.1 Human skin physiology

The outermost layer of human skin (10-15 micron) called stratum corneum which is primarily made of dead tissues. The next layer called epidermis (up to 50-100 micron), contains living cells and few nerves, but is devoid of blood vessels. Below the epidermis lies the third layer dermis (300-3000 micron) which contains both nerves and blood vessels. Beneath the dermis layer there is a layer of subcutaneous fat tissue that houses larger blood vessels and nerves [4].

2.2 Micro-needles

Two types of silicon micro-needles for insertion of fluid into the dermis layer (out-of-plane needle, length 250 micron) [Figure 1(a)] and into the subcutaneous fat layer (in-plane needle, length 3000 micron) [Figure 1(b)], were designed and studied. Both the micro-needles are designed with sharp wedge like tip angles to minimize skin resistance force and insertion pain. The range of the diameters of the blood corpuscles is from 2 μm (platelets) to about 15 μm (monocytes) [4]. Hence, to facilitate the passage of blood corpuscles, the bore diameter for the out-of-plane micro-needle is chosen to be 40 micron and the rectangular cross-section of the in-plane micro-needle is chosen to be 24×36 micron^2. The rectangular shape of the in-plane micro-needle body would provide almost 20% more mechanical strength to the needle than a

cylindrical needle of the same cross-sectional area, and thus reduce the bending of the needle. The choice of a rectangular cross-section is also favourable since it is technically more convenient to fabricate. The openings of the needle-channels have been designed to be on the side of the tip to prevent clogging of the channel by skin debris during insertion of the needle.

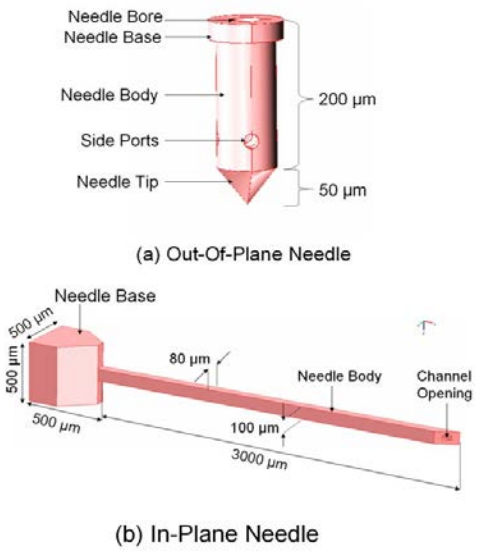

Figure 1: Structure and dimensions of the Out-of-plane and In-plane micro-needles

2.3 Micro-pump

The electrostatically actuated diaphragm pump consists of two chambers in series and three diffuser/ nozzle type elements to control the flow of fluid. Electric potentials applied at the electrodes cause vertical movement of the diaphragms and induces change of volume and fluid pressure in the pump chambers. Both of the pump chambers have a dimension of 1mm×1mm×50µm. The thickness of the diaphragm is 2µm and the separation between the diaphragm and the electrode is 10µm. The electrostatic 'pull-in' phenomena occur at an applied potential of about 35.4 volts.

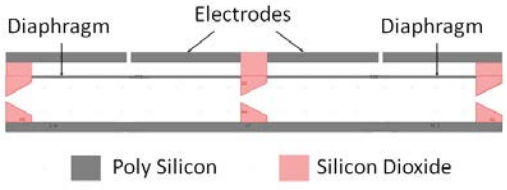

Figure 2: Electrostatically actuated micro-pump

3. Modeling using COMSOL

The 3D models of both the out-of-plane and in-plane micro-needles were created using COMSOL. In order to perform the structural analysis, we chose Application Modes> MEMS Module> Structural Mechanics> Solid, Stress-Strain from the "Model Navigator". The materials of both the needles were chosen to be polysilicon (Young's modulus E = 160 GPa, Poisson's ratio υ = 0.22, density ρ = 2320 Kg/m^3) from the "Subdomain Settings". The base planes of both the needles were considered to be fixed, while the rest of the needles were allowed to move freely. Theoretically human skin resistance is 3.18 MPa while penetrating the skin [1,5]. Once the skin has been penetrated, the pressure reduces to 1.6 MPa. When a Micro-needle enters the skin it experiences two kinds of forces: a) Buckling force and b) Bending force.

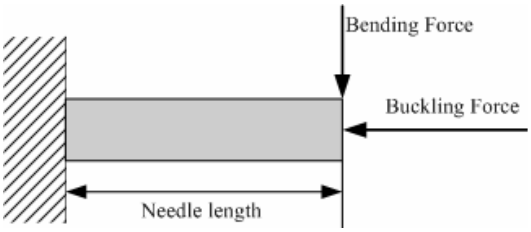

Figure 3: Modeling of the Micro Needle as cantilever

The Needle modeled as a cantilever is shown in the Figure 3. A compressive buckling force acts on the micro-needle in the axial direction. The maximum buckling force, which the micro-needle can withstand without breaking is given by [1,5]

$$F_{MaxBuck} = \frac{\pi^2 YI}{L^2} \qquad \text{(Eq.1)}$$

where, Y= Young's modulus, I= Geometric moment of inertia, L= Needle length.

The maximum free bending force that the micro-needle can withstand is given by [1,5]

$$F_{MaxFreeBend} = \frac{\sigma_y I}{cL} \qquad \text{(Eq.2)}$$

where, σ_y = yield stress of silicon (7 GPa) and c= distance of the outermost edge of the micro-needle from the neutral axis.

The bending force has a critical effect on fracture of silicon needle structure because of silicon's brittleness. When the strain of the tip is

close to the material yield strain, the structure fracture occurs.

The resistive force offered by the skin before the skin is punctured is given by [1,5]

$$F_{Skin} = P_{Piercing} A \qquad \text{(Eq.3)}$$

where, $P_{Piercing}$ = Pressure required to pierce the epidermis layer of skin = 3.18×10^{6} Pa.
A = cross-sectional area of the needle.
The values of $F_{MaxBuck}$, $F_{MaxFreeBend}$ and F_{Skin} for the out-of-plane needle were found to be 50N, 1.32N and 160 mN respectively. The same for the in-plane needle were calculated as 783.6 mN, 246.5 mN and 25.5 mN respectively. Since the maximum buckling force was substantially larger than the skin resistance force in both cases, the out-of-plane and in-plane micro-needles should be able to pierce the skin without breaking.

The fluidic analyses of the micro-needles were performed using the Navier-Stokes equations in the "Microfluidics" application mode of the "MEMS Module". The fluid (water) was modeled as incompressible, homogeneous and Newtonian.

For the sake of simplicity, the micro-pump was modelled in 2D geometry. The diaphragms and the electrodes were made of polysilicon, while silicon-dioxide was used as insulators between them. The analyses were performed in structural, electrostatic and fluid domains. Large deformation formulation was used and the mesh movement was described by the arbitrary Lagrangian-Eulerian (ALE) method. The space between electrodes was assumed to be filled by air (permittivity ε = 8.8542·10e-12 F/m) while the pumped fluid was assumed to be water, and modelled as incompressible, homogeneous and Newtonian.

4. Simulation Results

4.1 Simulation results and study of micro-needles

In the first step of simulation the maximum stress and deflection in the micro-needle structure were studied against different structural variables for both the out-of-plane and in-plane micro-needles. It was observed that for applied buckling force, the deformation of the structure was compressive in nature and the maximum stress was generated at the needle tips for the in-plane structure. But the region of maximum stress for the out-of-plane needle is around the side-ports. It was observed that the stress was dependent on the geometry of the side-ports. On application of bending force, the deformation was deflective from the needle-axes and maximum stress was produced near the needle base for both the needles.

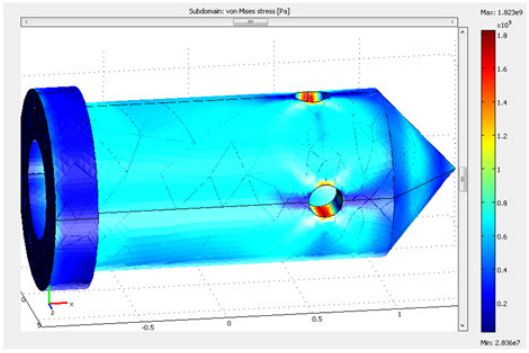

(a)

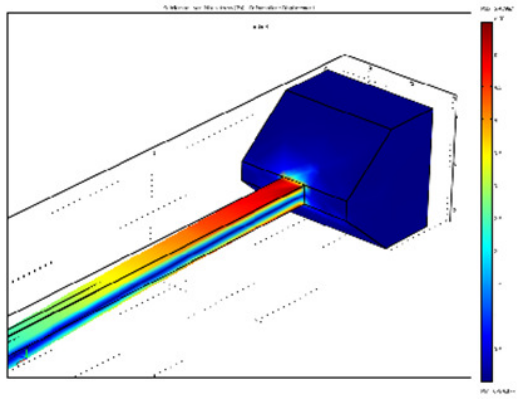

(b)

Figure 4 (a) and (b): Region of maximum stress in the out-of-plane and in-plane needles for buckling and bending forces respectively.

The next step was to study the maximum stress and deflection for different tip angles. It can be observed from Figure 5 (a,b) and 6 (a,b) that both the deflection and maximum stress decrease with increasing tip angle. This is expected since with the increment of the tip angle, the bending component of the applied force decreases, resulting in decrement of deflection and stress.

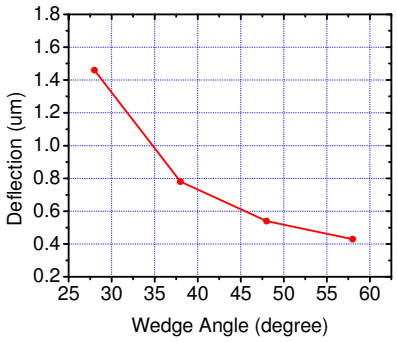

(a)

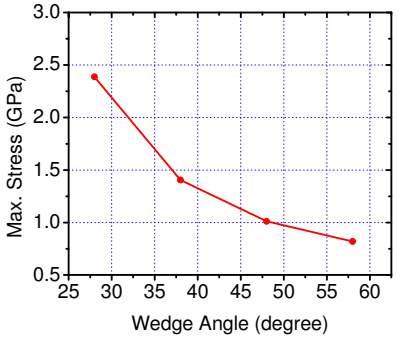

(b)

Figure 5 (a) and (b): Variation of deflection and maximum stress with tip angle for out-of-plane needle

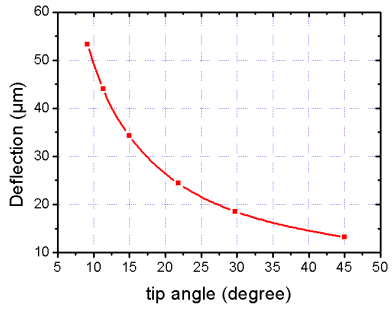

(a)

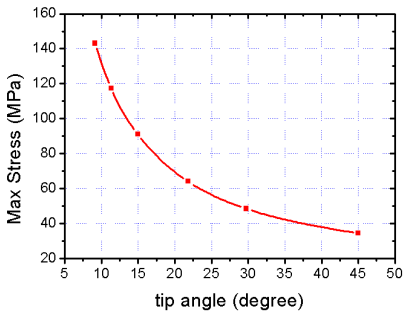

(b)

Figure 6 (a) and (b): Variation of deflection and Maximum stress with tip angle for in-plane needle

In the next step, the deflection, maximum stress and fluid flow rates through the needle channel under a constant pressure head was plotted for different cross-sectional area of the needle bore. It can be observed from Figure 7 (a) and (b) that the deflection, maximum stress and flow rate increases with increasing bore area. In case of the out-of-plane micro-needle, for a chosen bore diameter of 40µm the flow rate is almost 5µl/second and both the deflection and maximum stress are within tolerable limits. A similar study was performed for the in-plane micro-needle [Figure 8(a) and (b)], which allowed a flow rate of 0.064µl/second for the chosen bore area of 864µm^2. The area of the wedge shaped needle-tip decreases with increasing bore area, which in turn reduces the effective force acting on the needle-tip, since a fixed distributed load (pressure) is applied. However, both the deflection and maximum stress are within tolerable limits for the in-plane needle.

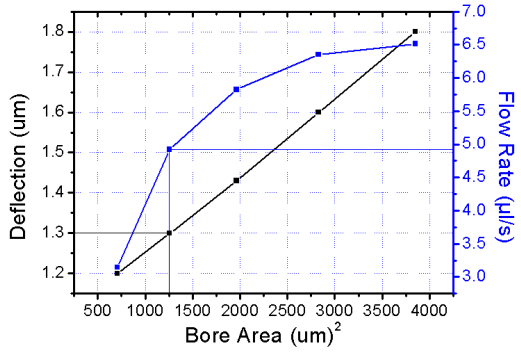

(a)

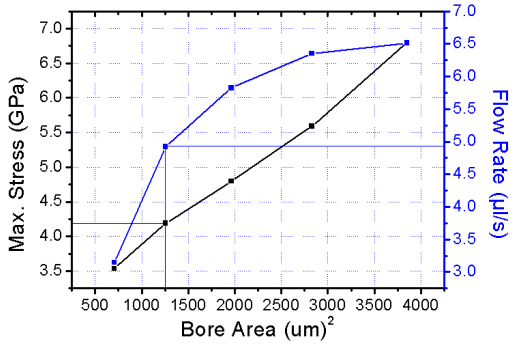

(b)

Figure 7 (a) and (b): Variation of deflection, maximum stress and flow rate with needle bore area for out-of-plane needle

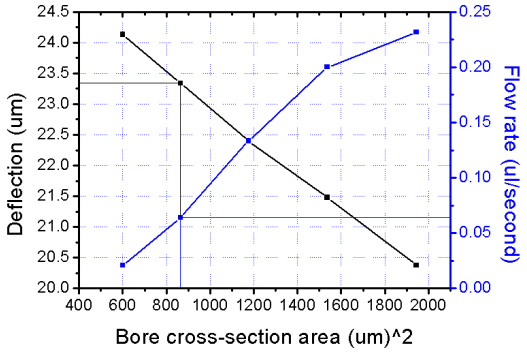

8(a)

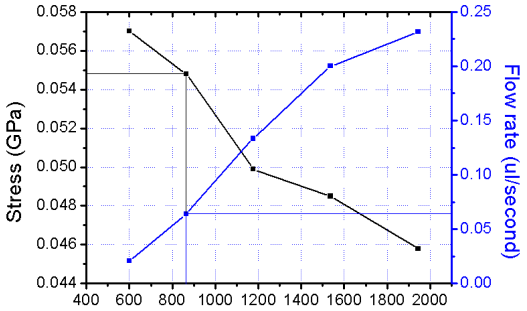

8(b)

Figure 8(a) and (b): Variation of deflection, maximum stress and flow rate with needle bore area for in-plane needle

4.2 Simulation results and study of micro-pump

The potential distribution in the electrostatically actuated micro-pump structure is shown in Figure 9. As the electrostatic pull-in of the diaphragm (the deflected diaphragm touches the electrodes) occurs at an applied potential of about 35.4 volts, the maximum operating voltage of the pump has been fixed at 32 volts. The deflection of the diaphragm with various applied voltages has been shown in figure 10.

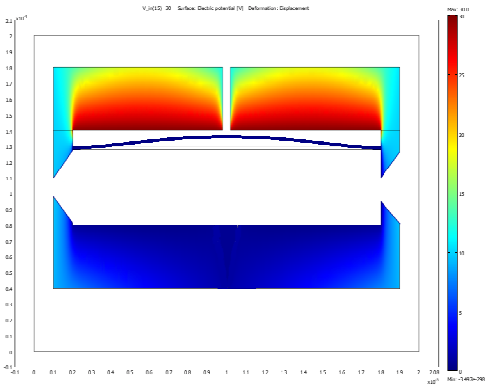

Figure 9: Potential distribution in a single chamber of the micro-pump

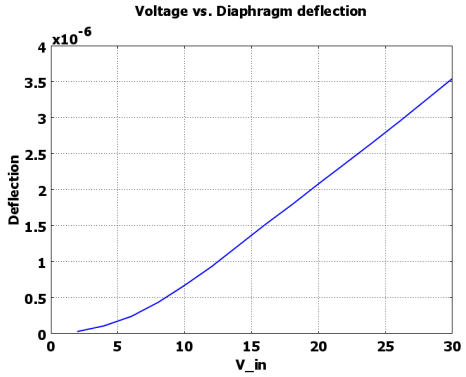

Figure 10: Variation of diaphragm deflection with applied potential

The diaphragm deflection due to an applied voltage of 32V is about 4µm, which causes a volume change of about 2.66 nl per stroke.

The 3D model of the pump diaphragm [Figure 11] is used to derive the frequency response of the membrane [Figure 13], from which the Eigen frequency of the membrane is obtained at about 31.1 KHz. The change of pump chamber volume per cycle will be maximum when it is operated at this frequency.

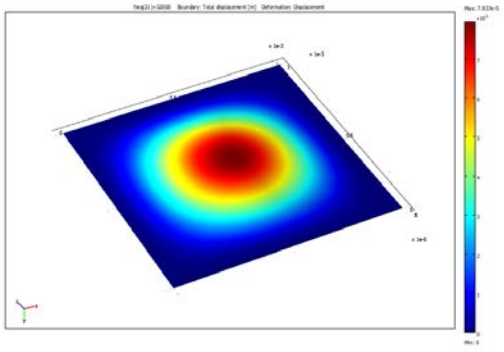

Figure 11: Deflected pump diaphragm

The microfluidic model of the pump was used to find the fluid velocity at the narrowest parts of the inlet nozzle and the outlet diffuser [6].

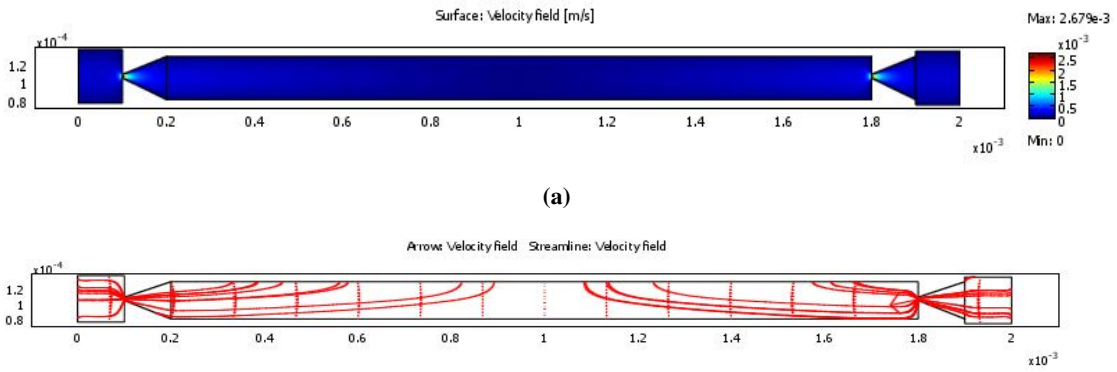

(a)

(b)

Figure 12: (a) Fluid velocity and **(b)** streamlines within a pump chamber when the diaphragm is pulled upward. The maximum fluid velocity occur at the narrowest parts of the nozzle/ diffuser elements.

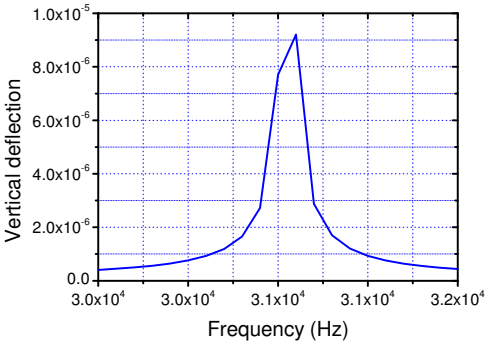

Figure 13: Frequency response of diaphragm deflection

The pressure drops across the nozzle and diffuser elements were also obtained from the fluidic model. These values were then used to find the pressure loss coefficients (ξ_n and ξ_d) of the nozzle and diffuser elements as given below.

$$\xi_n = 2.236 \times 10^3$$
$$\xi_d = 2.227 \times 10^3$$

The ratio of the pressure loss coefficients are [6],

$$\eta = \frac{\xi_n}{\xi_d} = 1.004$$

Now, the net pump volume flow rate at zero pressure across the pump is given by [6]

$$\phi = 2V_0 f\left(\frac{\sqrt{\eta}-1}{\sqrt{\eta}+1}\right) = 0.167\mu l$$

where, V_0 = maximum change of volume per stroke
= 2.66 nl
f = Eigen frequency = 31.1 kHz

The theoretically obtained pump volume flow rate was 167 nl/ second, which is appropriate for controlling the flow of microscopic volume of fluids.

5. Conclusions

This project work addresses the issues related to the design and simulation of MEMS based silicon micro-needles and micro-pump. It presents the analysis for the out-of-plane micro-needle that can be used for drug delivery and/or blood sampling from the dermis, and an in-plane micro-needle that is capable of inserting or extracting fluid from the subcutaneous fat layer. The bore areas for both the needles have been chosen to be large enough to allow passage of even the largest of the human blood corpuscles. The maximum buckling and bending forces that the micro-needle structures can withstand were calculated. Since the resistive force offered by the human skin was found to be significantly smaller than the maximum buckling and bending forces, it may be concluded that both the micro-needles are capable of penetrating the skin without breakage. Finally it can be established from simulation results that the deflection, maximum stress and fluid flow rates were

satisfactory for the chosen bore area of both the micro-needles.

An electrostatically actuated micro-pumping device was modeled and the data obtained from the numerical analysis were used to calculate the volume flow rate of the device. The electrostatic and microfluidic analyses provide valuable information regarding the working principle, actuation voltage, operating frequency and geometric parameters of the device. In order to maximize the volume flow rate, the pressure loss coefficient (η) should be maximized, which can be achieved by making the inlet nozzle much longer than the outlet diffuser. The ratio of nozzle and diffuser length, actuation voltage and frequency can be controlled independently to provide the optimum volume flow rate, which is appropriate in particular application scenario.

The micro-needle and micro-pump devices can be fabricated by photolithographic micro-fabrication techniques. Often an array of micro-needles is more appropriate than a single micro-needle for certain applications where larger volume of fluids is required to be inserted or extracted in a relatively short period of time. Since the micro-needle devices are dimensionally comparable to the micro-pump, the integration of both would allow the development of novel drug delivery systems. Such devices would also be capable of injecting multiple drugs simultaneously through the individually controllable pump and needle arrangements.

6. References

1. D.W. Bodhale, A. Nisar et al, Design, Fabrication and analysis of silicon microneedles for transdermal drug delivery applications, *Proceedings of the 3rd International Conference on the Development of BME,* 84-88(11-14th January, 2010).

2. A. Nisar, N. Afzulpurkar, B. Mahaisavariya, A. Tuantranont, MEMS-based micro-pumps in drug delivery and biomedical applications, *Sensors and Actuators B,130,* 917–942 (2008)

3. Peiyu Zhang, Colin Dalton et al, Design and fabrication of MEMS-based microneedle arrays for medical applications, *Microsystem Technology (DOI 10.1007/s00542-009-0883-5), 15,* 1073-1082 (2009).

4. Kim E. Barrett, Scott Boitano, Susan M. Barman, *Ganong's Review of Medical Physiology,* 23rd Edition (07-2009).

5. R. Sharaf, P. Aggarwal et al, On The Design of an Electronic Mosquito: Design and Analysis of the Micro-Needle, *International Conference on MEMS, NANO and Smart Systems (ICMENS'03),* (July 20-July 23, 2003).

6. A. Olsson, G. Stemme, E. Stemme, A valve-less planar fluid pump with two pump chambers, *Sensors and Actuators, A 46-47,* 549-556 (1995)

7. R. Zengerle, J. Ulrich, S. Kluge, M. Richter, A. Richter, A bidirectional silicon micropump, *Sensors and Actuators*, A 50, 81-86 (1995).

8. A. Nisar, Nitin Afzulpurkar, MEMS-based micropumps in drug delivery and biomedical applications, *Sensors and Actuators, B 130,* 917-942 (2008)

9. Tarik Bourouinay, Alain Bosseboeuf et al, design and simulation of an electrostatic micropump for drug-delivery applications, *J. Micromech. Microeng. 7,* 186-188 (1997).

7. Acknowledgements

COMSOL MULTIPHYSICS software was provided to the MEMS Design Center at the IRPEL through the National Program on Micro and Smart Systems (NPMASS), Govt. of India. Authors P. Podder and D. Mallick is receiving GATE fellowship from MHRD, Govt. of India.